

# Lawrence Berkeley National Laboratory

## Recent Work

**Title**

COLLIDING BEAM DETECTORS FOR THE SSC

**Permalink**

<https://escholarship.org/uc/item/4qv8q3dq>

**Author**

Trilling, G.H.

**Publication Date**

1986-10-01



# Lawrence Berkeley Laboratory

UNIVERSITY OF CALIFORNIA

## Physics Division

LBL 22384

Presented at the 3rd Theoretical Advanced Study  
Institute on Elementary Particle Physics (TASI-86),  
Santa Cruz, CA, June 23-July 18, 1986

COLLIDING BEAM DETECTORS FOR THE SSC

G.H. Trilling

October 1986

**TWO-WEEK LOAN COPY**

*This is a Library Circulating Copy  
which may be borrowed for two weeks.*



LBL-22384  
c.2

## **DISCLAIMER**

This document was prepared as an account of work sponsored by the United States Government. While this document is believed to contain correct information, neither the United States Government nor any agency thereof, nor the Regents of the University of California, nor any of their employees, makes any warranty, express or implied, or assumes any legal responsibility for the accuracy, completeness, or usefulness of any information, apparatus, product, or process disclosed, or represents that its use would not infringe privately owned rights. Reference herein to any specific commercial product, process, or service by its trade name, trademark, manufacturer, or otherwise, does not necessarily constitute or imply its endorsement, recommendation, or favoring by the United States Government or any agency thereof, or the Regents of the University of California. The views and opinions of authors expressed herein do not necessarily state or reflect those of the United States Government or any agency thereof or the Regents of the University of California.

## COLLIDING BEAM DETECTORS FOR THE SSC\*

George H. Trilling  
Lawrence Berkeley Laboratory  
and  
Department of Physics  
University of California, Berkeley, CA 94720

### 1. INTRODUCTION

There exists a reasonable amount of accessible literature on detectors for physics at 40 TeV.<sup>[1-3]</sup> In this brief report, therefore, I shall only summarize the considerations and refer the interested reader to the references for further detail. I want particularly to acknowledge my indebtedness to Ref. [3], which is the source of most of the figures in this paper.

One can represent the general requirements for detectors suitably matched to a high luminosity 40 TeV hadron collider in the following terms:

1. ability to detect and measure the directions and energies of quarks (jets), gluons (jets), leptons ( $e, \mu, \nu \dots$ ), and photons;
2. ability to handle high energies (fine segmentation, numerous absorption lengths, long magnetic paths, careful systematics);
3. ability to handle high luminosity (short signal collection times, fine segmentation, elaborate triggers, radiation hardness);
4. affordable, buildable and operable.

The high luminosity mentioned in item (3) extends to  $10^{33} \text{ cm}^{-2} \text{ s}^{-1}$ , and its need is presumably documented in the theoretical discussions in this volume and elsewhere.<sup>[1-4]</sup> For such luminosity, the estimated charged particle flux perpendicular to any surface, at a radial distance  $r_{\perp}$  from the beamline is shown in Fig. 1. Given the fact that radiation damage of electronics components becomes a major problem at levels of  $10^5$  to  $10^6$  rads ( $1 \text{ rad} = 3 \times 10^7 \text{ particles/cm}^2$ ), it is clear from Fig. 1 that vertex detectors (or other components) located close to the beam will probably be operable only at lower luminosities. It is worth noting, however, that

---

\*This work was supported in part by the U.S. Department of Energy under Contract No. DE-AC03-76SF0098.

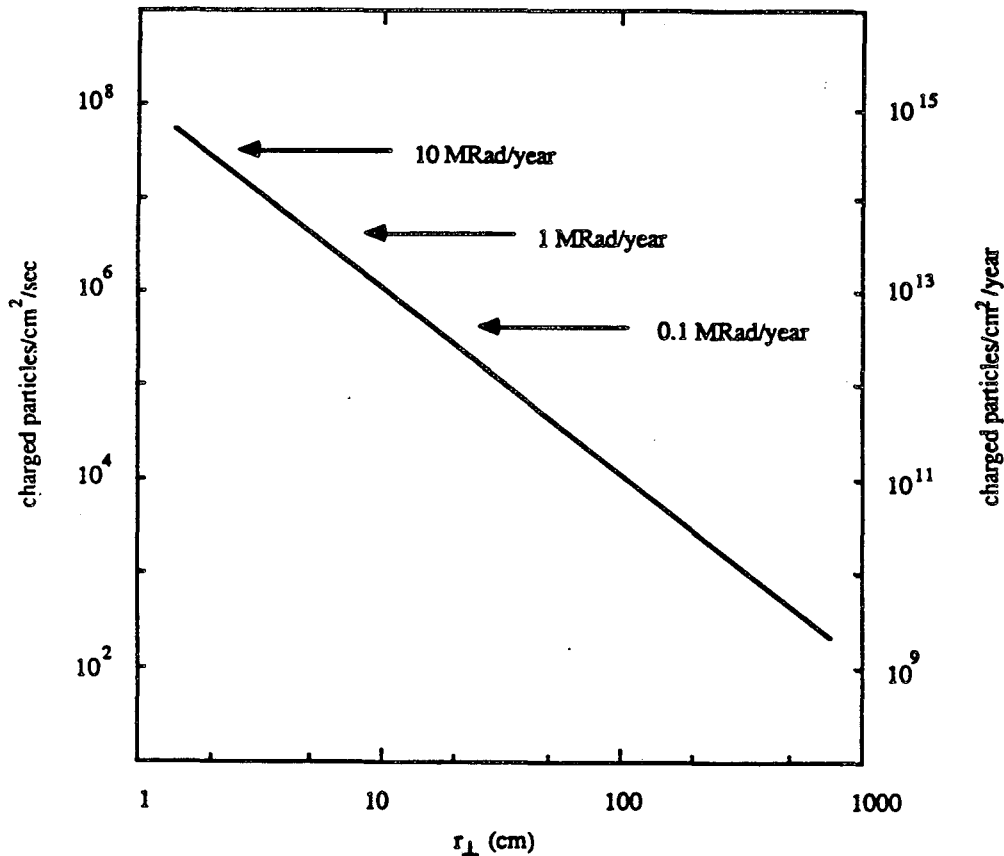


Figure 1: Charged particle rate per unit area perpendicular to the particle direction at  $L = 10^{33} \text{ cm}^{-2} \text{ s}^{-1}$ . Note that  $1 \text{ rad} = 3 \times 10^7 \text{ particles/cm}^2$ .

not all experiments on the SSC need be matched to the full  $10^{33} \text{ cm}^{-2} \text{ s}^{-1}$  luminosity. Thus, detectors focused on measurements near the forward direction may need relatively long interaction regions (perhaps  $\pm 100\text{m}$  rather than the nominal  $\pm 20\text{m}$  for high luminosity), and available luminosities in those areas will be correspondingly reduced. Hence even those components described in subsequent sections as capable of handling only somewhat lower luminosities may find application at the SSC.

A few comments about the SSC environment may be useful here. At full luminosity, the total interaction rate is about  $10^8 \text{ Hz}$ . The separation between bunches is  $4.8\text{m}$ , corresponding to a  $16\text{ns}$  time period between crossings. The average number of interactions per crossing is then 1.6. The bunch dimensions are about  $5\mu\text{m}$  radially and  $7\text{cm}$  longitudinally.

A typical detector for a  $40 \text{ TeV}$  collider will consist of many components to carry out the above enumerated requirements. In the rest of this report, I shall discuss in turn some of these components, and then shall briefly indicate how they might fit into a full detector.

## 2. TRACKING DETECTORS

### 2.1 General Considerations

By tracking, one usually means the accurate determination of the trajectories of most, or all, of the individual charged particles in an event. If this measurement is done in a magnetic field, both momenta and directions of the particles are obtained, whereas in the absence of a field only directions are determined. Existing collider detectors almost all have one or more drift chambers to serve as tracking devices. However, the increasing complexity of events at 40  $TeV$  raises some questions as to the usefulness of tracking devices, and the value of focusing on individual charged particles.

The principal functions of tracking devices in an SSC detector may be summarized as follows:

1. the matching of individual particle trajectories to energy deposits in calorimeter elements. This may be crucial for electron or muon identification;
2. the detection of secondary vertices from  $s$ ,  $c$ , or  $b$  quark decay or  $\tau$  lepton decay;
3. the identification of multiple  $pp$  interactions within a single bunch-bunch crossing;
4. the supplementation of energy flow information in regions where calorimeters have cracks;
5. the identification of unusual event topologies.

With a magnetic field, the momentum measurements can lead to improved electron identification, muon identification and the determination of effective masses of charged particle combinations. Furthermore, the determination of muon momenta may be crucial in the interpretation of the energy flow information from the calorimeters. However, the momentum precision at high energies is limited. For a drift chamber with magnetic field  $B$ , tracking length  $L$ , number of measuring layers  $N$  and spatial accuracy per layer  $\sigma_s$ , the fractional momentum precision has the dependence

$$\frac{\sigma_P}{P} \sim \frac{\sigma_s P}{BL^2 \sqrt{N}}$$

For  $\sigma_s = 200\mu\text{m}$ ,  $B = 1.5T$ ,  $L = 2\text{m}$ ,  $N = 100$ ,  $\sigma_P/P$  is about 30% at  $P = 1\text{ TeV}/c$ . Muons of higher momenta would have to be measured either in the absorber (see Section 4.2) or in a tracking system outside of the absorbers (similar to L3 at LEP).

## 2.2 Drift Chambers

Drift chambers, large and small, have been the tracking devices of choice in existing collider detectors. There is extensive experience and large systems have been built. No existing collider drift chamber, however, can adequately operate with the large luminosities under consideration here.

The large particle densities shown in Fig. 1 can be handled with reasonable performance and acceptable radiation damage effects only in tracking systems with very large numbers of wires and very small cell sizes (typically 5-10mm at large radii down to about 1-2mm at small radii). Numbers of channels are at least an order of magnitude greater than in existing detectors, and there are major mechanical problems connected with the support and stability of so many wires. At full luminosity, there will be, in addition to the event of interest, several others from the same or adjacent bunch crossings (collecting drifting electrons from 5mm requires typically 100ns, during which, at a luminosity of  $10^{33} \text{cm}^{-2} \text{s}^{-1}$ , about 10 interactions will have occurred). This may pose substantial problems for pattern recognition and large demands on computer time. These problems do not appear insuperable, but one has to say at this point that the feasibility of operating a large drift chamber at luminosities above  $10^{32} \text{cm}^{-2} \text{s}^{-1}$  is not established. The mechanical problems of holding so many wires will likely add material with the consequence that the chamber will contain 10-20% of a radiation length rather than the present typical 1-2%.

One of the most promising present ideas is to build a "straw" drift chamber.<sup>[6]</sup> Such a chamber consists of aluminized mylar "straws" of diameter  $\sim 3\text{mm}$ ; at the center of each straw, which acts as a cathode, is a sense wire. If the straws can be made into a rigid structure they would solve many of the existing problems: fewer wires to hold, ease of handling broken wires, etc.

## 2.3 Vertex and Other Tracking Detectors

For the detection of separated vertices, tracking detectors of very high spatial resolution are required, and they must be placed close to the interaction region to minimize the lever arm of the trajectory extrapolation. Silicon microstrip detectors with position resolutions of 5-10 $\mu\text{m}$  and two-particle separation capability at 100 $\mu\text{m}$  are being installed in the MARK II detector for SLC, and are under consideration for the CDF facility. The major problem for SSC applications appears to be radiation damage to the integrated electronics, since at a 5cm radius, the dose is about 1Mrad/year. In view of this problem it is not clear at present whether such detectors can be operated at luminosities beyond  $10^{31}$  to  $10^{32} \text{cm}^{-2} \text{s}^{-1}$ .

Another technology which has been proposed both for vertex detection and for the full-scale tracking capability is the use of bundles of scintillating plastic

or glass fibers of very small diameter ( $\lesssim 50\mu\text{m}$ ). Such a technique, employing fibers parallel to the beams, would have good spatial resolution, excellent two-track separation and possibly good radiation hardness. The major problems are the simultaneous achievement of small fiber diameters and long optical attenuation lengths, and the potentially long readout times if, for example, CCD's are used for the readout. Clearly much more R&D is needed to make this technology viable for high luminosity colliders.

### 3. CALORIMETRY

#### 3.1 General Considerations

The heart of almost any detector for a high energy, high luminosity collider is its collection of finely segmented calorimeters. These devices generally measure the charge or excitations produced by ionizing particles coming from either electromagnetic or hadronic showers, within small solid angle elements pointed at the interaction point. The showers are generated when high energy hadrons, photons or electrons impinge on the dense material within the calorimeter. Most calorimeters considered for the SSC application are of the sampling type, consisting of layers of dense material to produce the showers, separated by layers in which the ionizing particles are detected. The measurement of collected charge from a given shower provides a determination of the total energy of the particles which produced the shower.

The main functions of the calorimetry are the following:

1. measurement of electromagnetic and hadronic energy flow in each event as a function of direction;
2. identification of electrons and photons through their electromagnetic showers;
3. accurate measurement of electron energies
4. observation of missing transverse energy to flag energetic neutrinos or other non-interacting neutrals;
5. provision of analog information for a first level trigger.

Typically a calorimeter is divided into an upstream electromagnetic section and a downstream hadronic section. For the electromagnetic section, the typical dimension is the radiation length — hence thin plates and fine segmentation (see next section). For the hadronic part, the typical dimension is the interaction length — hence thicker plates and coarser segmentation. The hadronic section may be further subdivided into a precision upstream piece and a coarse downstream part, as a way of reducing costs without sacrificing too much performance.



## 3.2 Some Important Calorimeter Issues

### 3.2.1 Segmentation

The optimal segmentation is determined by three factors:

1. physics requirements such as the ability to determine jet-jet masses (to identify  $W$  or  $Z$ ), to identify leptons near jets, to determine missing transverse momentum and to separate  $\pi^0$  from  $\gamma$ ;
2. transverse shower sizes for both electromagnetic and hadronic showers;
3. cost — as one segments more finely, the number of electronics channels increases quadratically.

The Snowmass 86 calorimeter study group<sup>[6]</sup> suggests segmentation  $\Delta\eta\Delta\phi$  of  $0.03 \times 0.03$  for the electromagnetic section and  $0.06 \times 0.06$  for the hadronic section where  $\eta$  is the pseudo-rapidity and  $\phi$  the azimuth about the beam line. At a starting radial position of 1 to 2m, such a calorimeter is reasonably matched to both items (1) and (2). For a calorimeter which covers the central regions  $\eta = \pm 4$ , there are about 50K channels for one longitudinal readout. With three longitudinal readouts in both electromagnetic and hadronic calorimeters, there would be about 200K channels.

### 3.2.2 Energy Resolution

Typical achievable energy resolutions can be parametrized as follows:

$$\frac{\sigma_E}{E} = \frac{A}{\sqrt{E}} + B$$

where

$A \approx 0.1 - 0.2$  for electromagnetic section,

$\approx 0.5$  for hadronic section,

$B \approx 0.01$  with great care in the systematics.

To provide adequate longitudinal containment to achieve these resolutions at high energies requires about 25 radiation lengths (EM section) and 12 absorption lengths (hadronic section).

### 3.2.3 Compensation and Equalization

An important issue for hadronic calorimetry is the ratio between the responses to electrons and to hadrons of the same incident energies. Inequality of such response coupled with fluctuations, for a hadronic shower of fixed energy, in the

relative amounts of electromagnetic (from  $\pi^0$ ) and non-electromagnetic components, can lead, at high energies, to a much poorer resolution than suggested by the above formulas. This important effect is illustrated by the Monte Carlo calculation<sup>[6]</sup> embodied in Fig. 2.

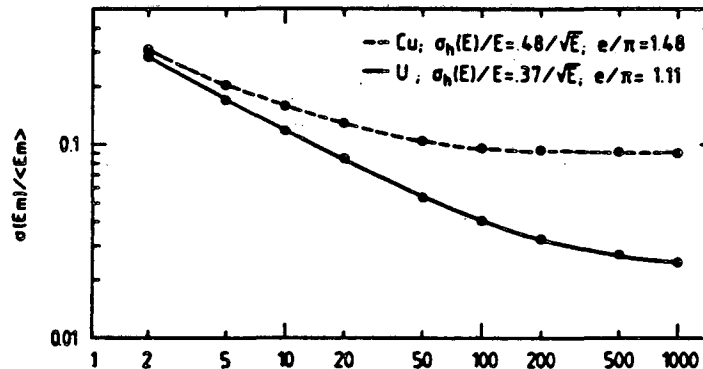


Figure 2: Monte Carlo calculations of the jet resolution for a thick  $4\pi$  calorimeter, for uncompensated ( $e/\pi = 1.48$ ) and nearly compensated ( $e/\pi = 1.11$ ) cases.

In conventional hadronic calorimeters with steel plates interspersed with detectors, the  $e/\pi$  ratio (ratio of signal from electrons relative to signal from  $\pi^\pm$  of the same energy) is about 1.5. This deviation from unity is mostly ascribed to effects of nuclear binding which reduce the ionization energy deposited in hadronic interactions. Both measurements and calculations<sup>[7]</sup>, however, indicate that ratios of  $e/\pi$  response are close to unity for calorimeters with high  $Z$  plates (lead, uranium) although the detailed mechanisms are complex and seem to involve both compensation (enhancement of hadronic response in uranium through fission) and equalization (reduction of electromagnetic response due to soft electron scattering and soft photon absorption in both lead and uranium). Uranium is more expensive and difficult to handle than lead, but provides greater compactness, and the compensation effect through fission.

### 3.2.4 Other Issues

Other desirable attributes of SSC calorimeters include the following:

1. speed of response — important in the association of signals with the appropriate event;
2. ease of calibration and stability. These will affect the systematic term  $B$  in Section 3.2.2;
3. uniformity of response of various calorimeter segments;

4. good linearity of response (to  $\gtrsim 5 \text{ TeV}$ );
5. hermiticity — absence of dead regions to maximize sensitivity to missing transverse momentum;
6. radiation hardness;
7. minimal cost for given performance.

### 3.3 Most Promising Calorimetry Techniques

From the previous discussion, the best techniques would involve the use of lead or uranium plates, interspersed with a radiation-hard, easily calibrated detecting medium. Liquid argon ionization detectors are the present favorites, and have been used in several electron-positron detector experiments. Liquid argon has a major drawback in the complexity of the cryogenics, and warm liquid calorimeters, presently under development for the UA1 detector, may prove to be a suitable replacement. The disadvantages of warm liquids are lower pulse heights, greater purity requirements and very limited experience. Yet another possibility is the use of thin silicon detectors as sampling devices. Experience is limited so far to small electromagnetic calorimeters, and the issues of cost, and feasibility of large devices need considerable study.

## 4. LEPTON IDENTIFICATION AND ENERGY MEASUREMENT

### 4.1 General Considerations

In this section, I shall be discussing the identification and measurements of electrons and muons. The physics goals toward which these measurements are aimed include the following:

1. the search for new, more massive  $W$ 's and  $Z$ 's;
2. the detection of standard  $W$ 's and  $Z$ 's;
3. the detection of  $b$ ,  $t$  and more massive quarks;
4. the correction of calorimetry measurements for fast muons which usually traverse the calorimeter without depositing most of their energy;
5. the association of missing  $P_T$  with neutrinos rather than new non-interacting neutrals.

Clearly many of these goals strike at the heart of the physics justifications for high energy hadron colliders. The devices appropriate for electrons and muons are very different, and their systematics are also very different. It is therefore

usually desirable to have both muon and electron identification capability, even for measurements in which only one may appear necessary.

Typically discrimination against hadrons is required at the  $10^{-3} - 10^{-4}$  level depending on the processes and the kinematic region under study.

#### 4.2 Measurement of Muons

Muons are identified through their penetration of large thicknesses of absorbing material, including the various calorimeters, generally followed by additional plates of steel. Roughly speaking, 100  $GeV/c$  hadrons have about  $10^{-3}$  punchthrough probability in traversing 5 meters of steel, where punchthrough probability is defined as the probability that one or more particles are detected at a given longitudinal position in the absorber.<sup>[3]</sup> This probability goes to about  $6 \times 10^{-3}$  for 500  $GeV/c$  hadrons and increases by another factor of 1.5-2 for a reduced steel thickness of 4 meters. With measurements of exit position and direction of the muon candidates, and sampling of their trajectories within the absorber, these probabilities can be reduced by factors as high as 100. Misidentification can also arise from  $\pi$  and K decay in flight, although these effects should not be large at the highest momenta. Actual contributions at the lower momenta will depend on how effectively the tracking system can recognize decays in flight.

Figure 3 shows the main contributions to muon energy loss in iron as a function of energy. It is worth noting that, at energies above 400  $GeV$ , pair production and bremsstrahlung dominate the total loss.

Muon energy can only be measured through tracking in a magnetic field. As indicated earlier, such measurements up to 1  $TeV/c$  can be done in a large central drift chamber immersed in a magnetic field. Alternatively (or in addition), muon momenta can be measured in the steel absorber if it is magnetized and longitudinally segmented so that tracking detectors can be inserted about every 50 to 100cm. For 5 meters of magnetized steel with a field of 2T, the multiple scattering contribution to the momentum error is about 10% (and varies inversely with the square root of the magnetized steel thickness). From the formula in Section 2.1, if we assume a  $300\mu m$  position accuracy, a measurement every 50cm over a path of 5m, and a 2T field, we find fractional measurement errors of about 15% at 1  $TeV/c$ , and 30% at 2  $TeV/c$ . The electromagnetic energy loss fluctuations in the iron are relatively small by comparison, but the confusion in the detectors due to extraneous shower tracks may make the assumed  $300\mu m$  accuracy optimistic. Combination of central tracker information and absorber tracking measurements can substantially reduce the momentum errors at the highest momenta.

#### 4.3 Measurement of Electrons

Precise electron energy measurements can be done in a straightforward way

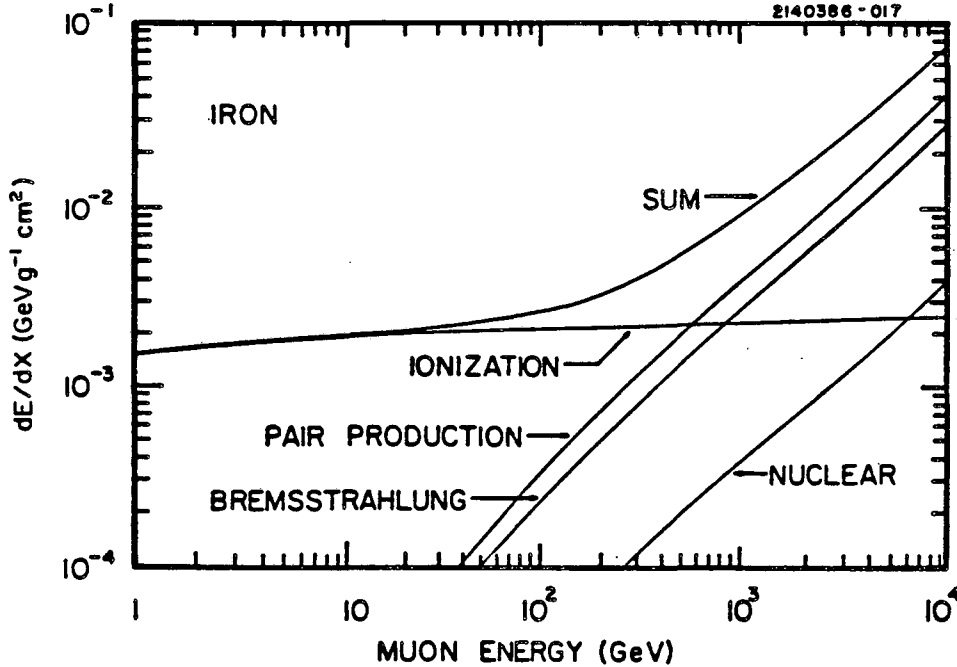


Figure 3: The various components of muon energy loss in iron.

in an electromagnetic calorimeter. As indicated in Section 3.2, at energies above 100 GeV the precision should be at the 1-2% level and will be principally limited by the ability to control the systematics. Another limitation for electrons close to jets will be the ability of the segmented calorimeter to separate the contributions of the electron from those of nearby shower particles.

Figure 4 summarizes various techniques for electron identification and their ranges of applicability, as indicated by the solid lines. The lower two lines are based on the calorimetry; and, in addition, the lowest line also uses momentum information from the central tracking detector. Transition radiation detectors consist of large numbers of thin dielectric foils or fibers, for example CH<sub>2</sub>, separated by very small gaps. Relativistic particles traversing the foils emit photons in the energy regime of order  $\gamma$  times the foil material plasma frequency (about 20 eV). These photons are usually detected in xenon proportional chambers behind the foils. Pion rejections of order 10<sup>-2</sup> may be achievable in the energy range from 1 to a few hundred GeV to supplement the 10<sup>-3</sup> rejection expected from calorimetry.

The other techniques shown in Fig. 4 are based on various methods of detecting synchrotron photons radiated by electrons bent in the large magnetic field of a central tracking detector. Again, these methods could supplement the rejection offered by calorimetry.

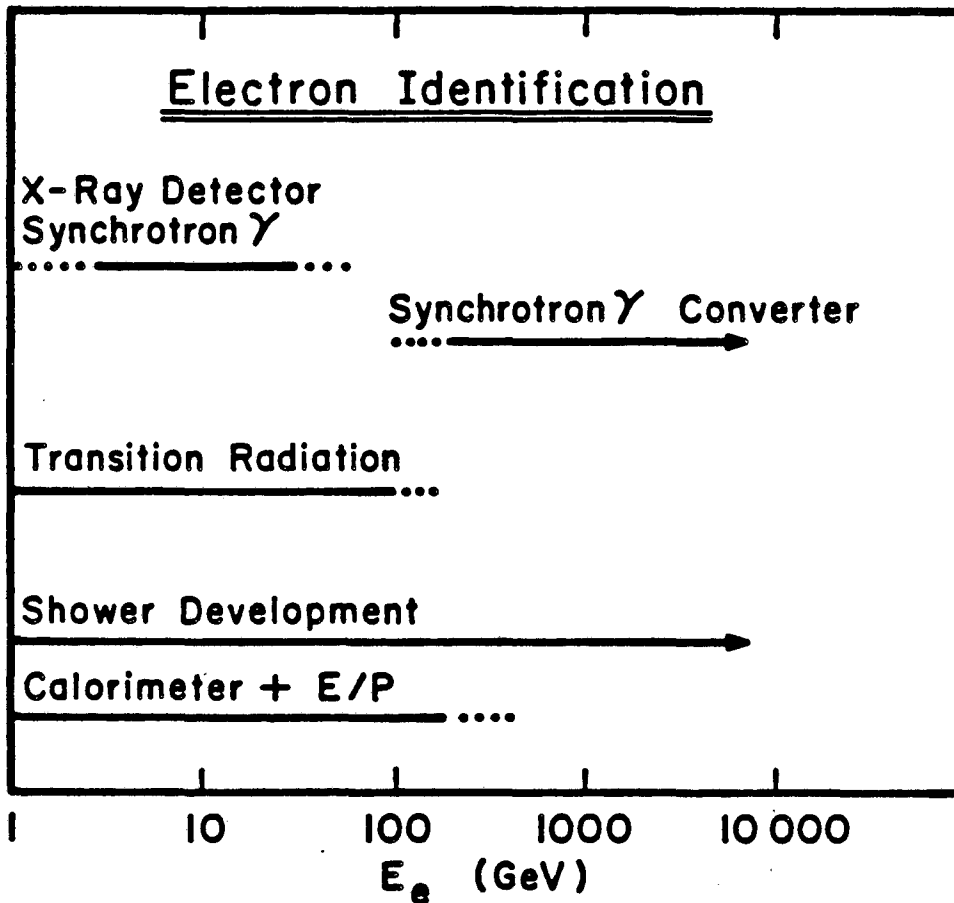


Figure 4: Summary of the energy range of various techniques for electron identification.

## 5. TRIGGER

With a luminosity of  $10^{33} \text{ cm}^{-2} \text{ s}^{-1}$  and an estimated inelastic cross-section of 100mb, the raw event rate is  $10^8 \text{ Hz}$ . One wants to record data at a rate which (1) is much greater than the rate of interesting events, but (2) does not overwhelm the recording medium or the off-line computer capability. This rate is usually taken to be a few Hz. Thus the task of the trigger is to go from the  $10^8 \text{ Hz}$  raw rate to the few Hz recording rate without loss of interesting physics. This rather technical problem has been the subject of a recent workshop at Fermilab<sup>[8]</sup> and I only make a few comments here.

The trigger strategy might consist of a hierarchy of three successively more sophisticated trigger levels:

1. a first level based on analog calorimetric information, requiring about  $1\mu\text{s}$  processing time, with a rejection capability of order  $10^3 - 10^4$  (high  $P_T$  electron candidates or jets, large missing  $P_T$ , etc.);
2. a medium level requiring more complicated combinations of information with about  $10\mu\text{s}$  processing time and rejection capability of roughly  $10^2$  (isolated electrons, various combinations of jets, muons tracked in absorber, etc.);
3. a third level involving a processor farm to reconstruct tracking information. The rejection might be another factor of  $10^2$ .

In this system, only the accepted triggers of level  $N$  are sent to level  $N + 1$  for additional processing. There is an important element here which differs from existing systems. The time between beam crossings (15ns for the SSC) is short compared to the first level trigger processing time ( $1\mu\text{s}$ ). This implies that the full data for every channel and for every crossing must be stored until its trigger information is available. Figure 5 shows a model of the data flow in such a system as discussed by Lankford and Dubois<sup>[8]</sup> in the Fermilab Workshop Proceedings.

The issue of off-line computing needs and how one might hope to meet them is also of importance. With the expected event complexity, an event rate of 1Hz from one detector is estimated to require about  $10^3$  VAX-11/780 equivalents to keep up with the production processing. This does not include the physics analyses, Monte Carlo's and program development time. A model for a possible Central Computing Facility to meet these requirements is shown in Fig. 6. Again, more details are available in the Fermilab Workshop Proceedings.

## 6. A $4\pi$ DETECTOR

I conclude this discussion of detectors for a 40  $T\text{eV}$  collider by showing in Fig. 7 a schematic diagram of a  $4\pi$  detector considered in a cost-estimating exercise for an initial SSC detector complement.<sup>[9]</sup> The picture is virtually self-explanatory, and the scale is clearly indicated. There are about 700K channels of electronics with 240K in various drift chamber tracking systems, 280K in the calorimetry and 180K in the muon system. The estimated cost is of order \$ 300M. This is not a real detector design, optimized to provide maximum performance for given cost, but it does indicate the general magnitude of the experimental devices. It should be emphasized that some of the detectors appropriate for the SSC will undoubtedly be more modest and more specialized — my example is at the high end of the range of complexity and cost.

I conclude with a remark about the sociology of a physics effort on so large a scale. It will take very large teams, with excellent coordination, to build and oper-

ate such detectors, and to exploit the physics from them. The physics objectives, however, are exciting and imperative. I am sure that as soon as construction of the SSC is approved, experimenters from all over the world will quickly put together the teams needed to begin design and construction.

## REFERENCES

- [1] *Proceedings of the 1984 Summer Study on the Design and Utilization of the Superconducting Super Collider*, edited by R. Donaldson and J.G. Morfin, (Snowmass, Colorado, 1984).
- [2] *Proceedings of the ECFA-CERN Workshop on Large Hadron Colliders in the LEP Tunnel* (1984).
- [3] Report of the Task Force on Detector R&D for the Superconducting Super Collider, SSC-SR-1021 (1986).
- [4] E. Eichten, I. Hinchliffe, K. Lane and C. Quigg, *Rev. Mod. Phys.* **56**, 579 (1984).
- [5] Proceedings of the 1986 Summer Study on the Design and Utilization of the Superconducting Super Collider, to be published.
- [6] T. Akesson et al., *NIM A* **241**, 17 (1985).
- [7] *Proceedings of the Workshop on Compensated Calorimetry*, (California Institute of Technology, 1985).
- [8] *Proceedings of the Workshop on Triggering, Data Acquisition and Computing for High Energy/High Luminosity Hadron-Hadron Colliders*, edited by B. Cox, R. Fenner and P. Hale (Fermilab, 1985).
- [9] Cost Estimate of Initial SSC Experimental Equipment, SSC-SR-1023 (1986).



### General Model of Data Flow

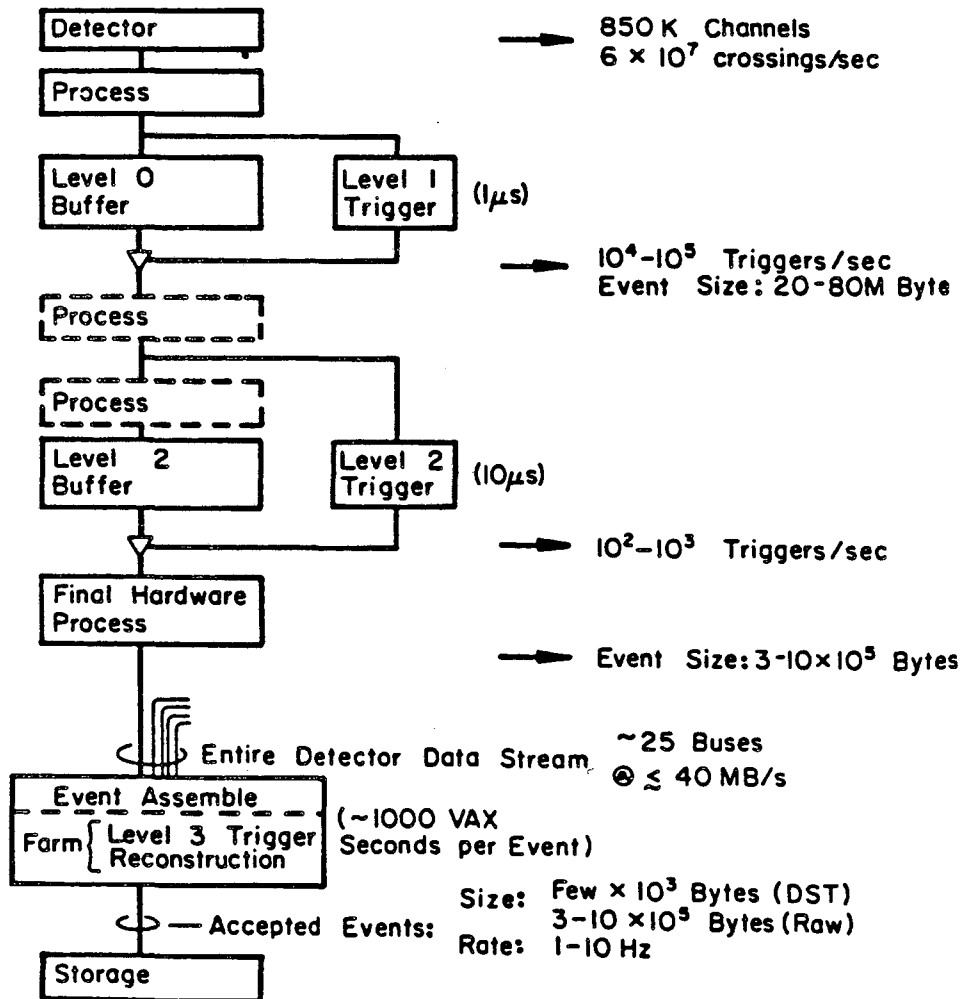


Figure 5: Flow diagram of data from detector to permanent storage.

**SSC  
MODEL FOR CENTRAL COMPUTING**

In this model, permanent data storage is done at each IR, and the recording media are manually transported to the Central Facility.

This diagram shows the logical structure but not the actual bus structure. The Farm Manager and Analysis computer are hoped to be as compatible as possible, and may not be distinct physical units.

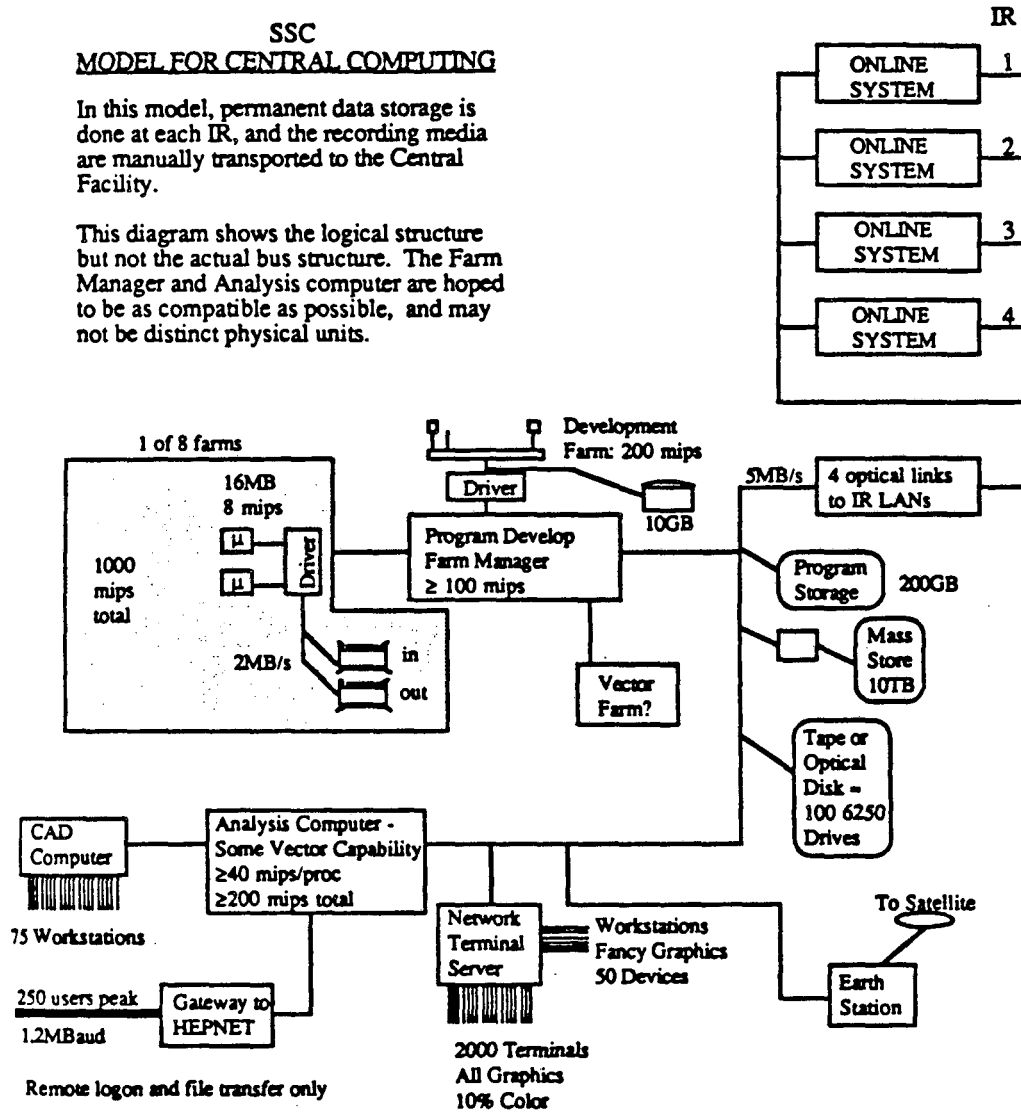


Figure 6: Conceptual Model of SSC central off-line computing facility.

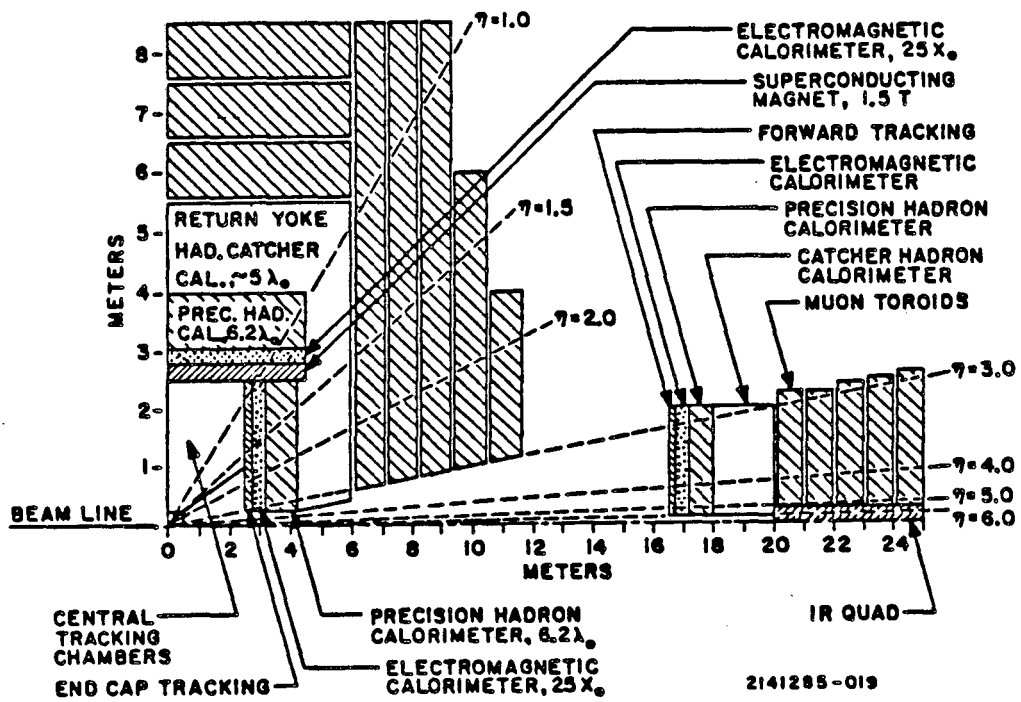


Figure 7: Schematic diagram of 4π Detector for SSC.

This report was done with support from the Department of Energy. Any conclusions or opinions expressed in this report represent solely those of the author(s) and not necessarily those of The Regents of the University of California, the Lawrence Berkeley Laboratory or the Department of Energy.

Reference to a company or product name does not imply approval or recommendation of the product by the University of California or the U.S. Department of Energy to the exclusion of others that may be suitable.

*LAWRENCE BERKELEY LABORATORY  
TECHNICAL INFORMATION DEPARTMENT  
UNIVERSITY OF CALIFORNIA  
BERKELEY, CALIFORNIA 94720*